LIMNOLOGY and OCEANOGRAPHY

ASLO

Limnol. Oceanogr. 9999, 2024, 1–15

doi: 10.1002/lno.12555

Multiple biotic interactions establish phytoplankton community structure across environmental gradients

Stephanie Dutkiewicz,[1,2*] **Christopher L. Follett**,[1,3] **Michael J. Follows**,[2] **Fernanda Henderikx-Freitas**,[4] **Francois Ribalet**,[5] **Mary R. Gradoville**,[6] **Sacha N. Coesel**,[5] **Hanna Farnelid**,[7] **Zoe V. Finkel**,[8] **Andrew J. Irwin**,[9] **Oliver Jahn**,[1] **David M. Karl**,[4,10] **Jann Paul Mattern**,[11] **Angelicque E. White**,[4,10] **Jonathan P. Zehr**,[11] **E. Virginia Armbrust**[5]

[1]Department of Earth Atmosphere and Planetary Sciences, Massachusetts Institute of Technology, Cambridge, Massachusetts, USA
[2]Center for Global Change Sciences, Massachusetts Institute of Technology, Cambridge, Massachusetts, USA
[3]Department of Earth, Ocean and Ecological Sciences, University of Liverpool, Liverpool, UK
[4]Department of Oceanography, University of Hawaii at Mānoa, Honolulu, Hawaii, USA
[5]School of Oceanography, University of Washington, Seattle, Washington, USA
[6]Columbia River Inter-Tribal Fish Commission, Portland, Oregon, USA
[7]Centre for Ecology and Evolution in Microbial Model Systems, Linnaeus University, Kalmar, Sweden
[8]Department of Oceanography, Dalhousie University, Halifax, Canada
[9]Department of Mathematics and Statistics, Dalhousie University, Halifax, Canada
[10]Daniel K. Inouye Center for Microbial Oceanography: Research and Education, University of Hawaii at Mānoa, Honolulu, Hawaii, USA
[11]Ocean Sciences Department, Institute of Marine Sciences, University of California, Santa Cruz, Santa Cruz, California, USA

Abstract

The combination of taxa and size classes of phytoplankton that coexist at any location affects the structure of the marine food web and the magnitude of carbon fluxes to the deep ocean. But what controls the patterns of this community structure across environmental gradients remains unclear. Here, we focus on the North East Pacific Transition Zone, a $\sim 10^{\circ}$ region of latitude straddling warm, nutrient-poor subtropical and cold, nutrient-rich subpolar gyres. Data from three cruises to the region revealed intricate patterns of phytoplankton community structure: poleward increases in the number of cell size classes; increasing biomass of picoeukaryotes and diatoms; decreases in diazotrophs and *Prochlorococcus*; and both increases and decreases in *Synechococcus*. These patterns can only be partially explained by existing theories. Using data, theory, and numerical simulations, we show that the patterns of plankton distributions across the transition zone are the result of gradients in nutrient supply rates, which control a range of complex biotic interactions. We examine how interactions such as size-specific grazing, multiple trophic strategies, shared grazing between several phytoplankton size classes and heterotrophic bacteria, and competition for multiple resources can individually explain aspects of the observed community structure. However, it is the combination of all these interactions together that is needed to explain the bulk compositional patterns in phytoplankton across the North East Pacific Transition Zone. The synthesis of multiple mechanisms is essential for us to begin to understand the shaping of community structure over large environmental gradients.

Phytoplankton are single-celled microscopic photosynthesizing organisms that play important roles as the base of the marine food web and are a key component of Earth's carbon cycle. These organisms are extremely diverse, spanning many orders of magnitude in size and playing different roles in biogeochemical cycles. Different communities of phytoplankton (defined here as the

*Correspondence: stephd@mit.edu

Additional Supporting Information may be found in the online version of this article.

Author Contribution Statement: SD and MJF conceived the idea for the study, FHF, FR, MRG, HF, AEW, JZ, DMK, and EVA supplied observational data and insight, SD, CLF, and MJF developed the theory, OJ and SD developed the model, SD conducted the simulations, SNC, JPM, ZVF, and AJI provided valuable context, SD wrote the paper with input from all co-authors.

combinations of coexisting types) occur over a wide range of spatial and temporal scales in the ocean (Margalef 1978; Aiken et al. 2009; Fremont et al. 2022), support a variety of food webs, and have diverse roles in the carbon cycle (Fuhrman 2009; Guidi et al. 2009; Cermeño et al. 2016). Observations have offered insights into the global scale biogeography of different phytoplankton functional types, including different types of picophytoplankton (e.g., Flombaum et al. 2013; Flombaum et al. 2020), nitrogen fixers (e.g., Tang and Cassar 2019), diatoms (e.g., Tréguer et al. 2018), as well as aspects of community structure such as cell size (e.g., Acevedo-Trejos et al. 2018). In an attempt to understand these biogeographies, several studies have examined mechanisms, including biotic interactions such as grazing pressure or competition for limiting nutrients, to explain the geographical patterns of specific functional types (e.g., nitrogen fixers, Ward et al. 2013; Schlosser et al. 2013) or the size structure of the population (Armstrong 1999; Banas 2011; Ward et al. 2014). These studies have, in general, focused on a single group of organisms (e.g., nitrogen fixers) or one aspect of community structure (e.g., size distribution) and have examined one underpinning mechanism (e.g., role of grazing pressure) at a time to help explain the observed patterns across environmental gradients. However, phytoplankton communities are diverse, comprising various taxa, and it is likely that multiple mechanisms occur simultaneously at any given location. Here, we explore the necessity of multiple biotic interactions together to understand observed biogeographical patterns and, in particular, the intricate community structures observed transitioning between oligotrophic and eutrophic conditions. We capitalize on data collected during three cruises in the North East Pacific Transition Zone to both describe observed community structure across environmental gradients and provide a conceptual and theoretical interpretation of the combination of several mechanisms that control these patterns.

The North East Pacific Transition Zone is an area of approximately 10° in latitude stretching from the warm, oligotrophic waters of the subtropical gyre to the cold, nutrient-replete, subpolar gyre. Within this transition zone, satellite imagery and several field expeditions have shown large gradients in chlorophyll *a* (Chl *a*) (Fig. 1a–c), sea surface temperature (Fig. 1d), nutrients (e.g., nitrate and nitrite, Fig. 1e) and in related biogeochemical and ecosystem variables (Polovina et al. 2001; Church et al. 2008; Kavanaugh et al. 2014; Follett et al. 2021). These gradients persist, though they shift seasonally (Follett et al. 2021). Surface waters moving southeast from the subpolar gyre across this region have nutrients removed by the export of organic matter through the wintertime mixed layer (Follett et al. 2021), leading to large gradients in the rate at which nutrients are supplied to the sunlit layer (Fig. 1f). Strong shifts in phytoplankton communities are observed by many expeditions across this transition zone, with the south dominated by picophytoplankton and the north by larger autotrophs (e.g., Bogorov 1958; Endo et al. 2018; Juranek et al. 2020; Xu et al. 2022). However, observations obtained during three cruises across the North East Pacific Transition Zone in the spring/early summer of 2016, 2017, and 2019 (we will refer to these cruises as G1, G2, and G3) along a meridional transect at 158°W (Fig. 1) revealed more complex spatial successions of phytoplankton than just a shift in the average size of the community. Moving northward, data from these cruises show a sharp increase in some pico- and nanoplankton across this region (Juranek et al. 2020) and sharp declines in both nitrogen-fixing bacteria (Gradoville et al. 2020) and the smallest autotroph *Prochlorococcous* (Follett et al. 2022).

In this study, we first describe the broad-scale patterns of size structure and taxonomic patterns that were consistent across the three cruises. Our goal is to identify the mechanisms that set these distribution patterns, not of a single group of organisms, but of several phytoplankton groups that together form the majority of the community. We use simple ecological theory together with a complex global/ecosystem model to show that a combination of biotic interactions is needed to explain the bulk compositional patterns in phytoplankton across the North East Pacific Transition Zone: these include size-based growth and grazing, changing lengths of trophic chains, and stoichiometric constraints. This same set of interactions is likely to be relevant over large swaths of the ocean where there is a strong gradient in resource supply rates.

Methods

Observations from three cruises

As part of the Simons Collaboration on Ocean Processes and Ecology (SCOPE) project, three SCOPE-Gradients cruises (G1, G2, and G3) transited from the oligotrophic waters off Hawaii northward along 158°W and returned along the same longitude (Fig. 1). G1 took place in April and May 2016; G2 in May and June 2017; and G3 in April 2019. Each cruise collected a wide variety of ecological and biogeochemical data, and many results have been discussed in previous publications (Björkman et al. 2018; Gradoville et al. 2020; Juranek et al. 2020; Pinedo-Gonz´alez et al. 2020; Heal et al. 2021; Allen et al. 2022; Boysen et al. 2022; Carlson et al. 2022; Lambert et al. 2022; Graff van Crevel et al. 2023; Park et al. 2023). For the purposes of this study, we focus on latitudinal patterns of Chl *a*-containing organisms as measured by three optical instruments (Supporting Information Fig. S1) and molecular techniques from water collected near the surface either from the ship's underway intake or from conductivity, temperature, depth sensor casts.

Continuous underway flow-cytometer (SeaFlow) was used in all three cruises to estimate the biomass of small-size phytoplankton, nominally 0.5–3 μm in diameter. These data were classified into four different populations: the picocyanobacteria *Prochlorococcus* and *Synechococcus*, small eukaryotes, and the diazotroph *Crocosphaera* (Fig. 2b–d; Supporting Information Figs. S2, S3). In addition, the data was divided into biomass within specific size bins (Supporting Information Fig. S4).

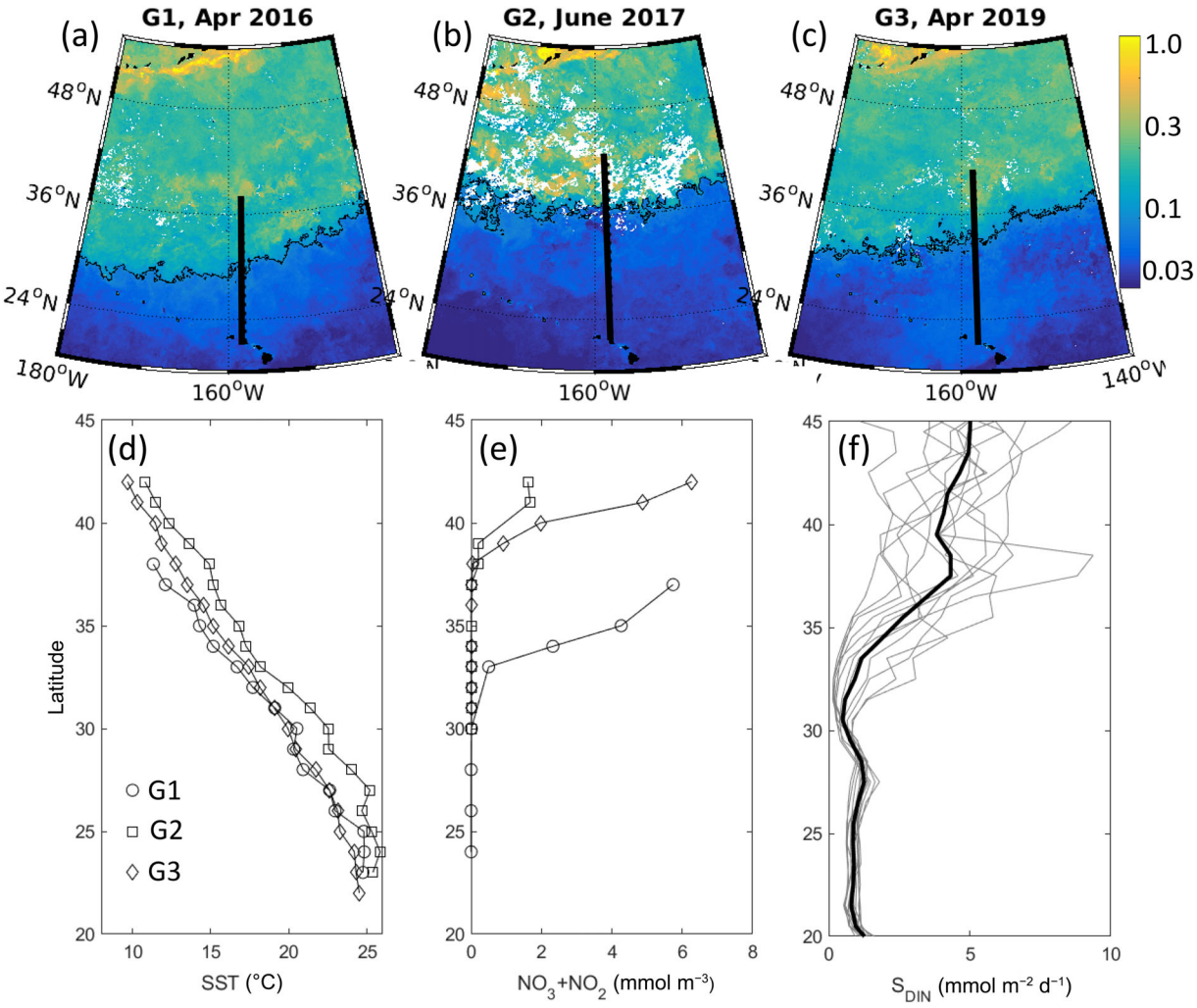

Fig. 1. Environmental context of three SCOPE-Gradients cruises (G1–G3): (**a–c**) NASA MODIS-Aqua Satellite estimate of monthly mean Chl *a* (mg m^{-3}), with cruise tracks superimposed (**a**) G1, Apr 2016; (**b**) G2, June 2017; (**c**) G3, Apr 2019; (**d**) sea surface temperature (°C) from each cruise; (**e**) nitrate + nitrite (mmol N m^{-3}) from each cruise; (**f**) flux of dissolved inorganic nitrogen into the top 50 m (mmol N m^{-2} d^{-1}) from the numerical model. For (**a**)–(**c**), the black contour is 0.1 mg Chl m^{-3}. For (**d**) and (**e**) circles indicate G1, squares G2, and diamonds G3. In (**f**), the modeled rates include supplies by vertical and horizontal transport, vertical mixing, and from remineralization from organic matter by heterotrophic organisms. Gray lines in (**f**) are monthly means, and thicker black line is the annual average.

Imaging FlowCytobot (IFCB; McLane Labs) was used to estimate the size and taxonomy of phytoplankton cells, from ~ 3 to 100 μm in diameter (Supporting Information Fig. S5).

We use these observations to determine the total biomass of diatoms (Fig. 2f) and the non-rare maximum-sized phytoplankton at each latitude (Fig. 2a). However, IFCB data are only available for G2. A laser in situ scattering and transmissometry sensor (LISST 100-X; Sequoia Scientific Inc.) was used for all three cruises to estimate particle size distributions between ~ 1.25 and 100 μm (Supporting Information Fig. S4). For further details of these measurements, assumptions, and conversions to biomass, *see* Ribalet et al. (2019), White et al. (2015), Juranek et al. (2020), and Supporting Information Text S1.1.

Nitrogen-fixing diazotrophs are important biogeochemical components of the phytoplankton, but the most dominant type observed along the transition zone, the UCYN-A1/haptophyte symbiosis (Gradoville et al. 2020), cannot (as yet) be identified optically. Here, we used discrete DNA samples to provide patterns of *nifH* gene abundances of this group (Fig. 2e). For more details on the methodology used, *see* Gradoville et al. (2020) and Supporting Information Text S1.2.

Theoretical framework

Ecological theories reduce a system of interest to the simplest possible components and interactions needed to explain a specific phenomenon. Here, we consider several planktonic interactions that we believe are at play in setting community structure in the transition zone and consider each of five "mechanisms" individually (labeled A–E, Fig. 3). In the theoretical frameworks, we consider the biomass of phytoplankton

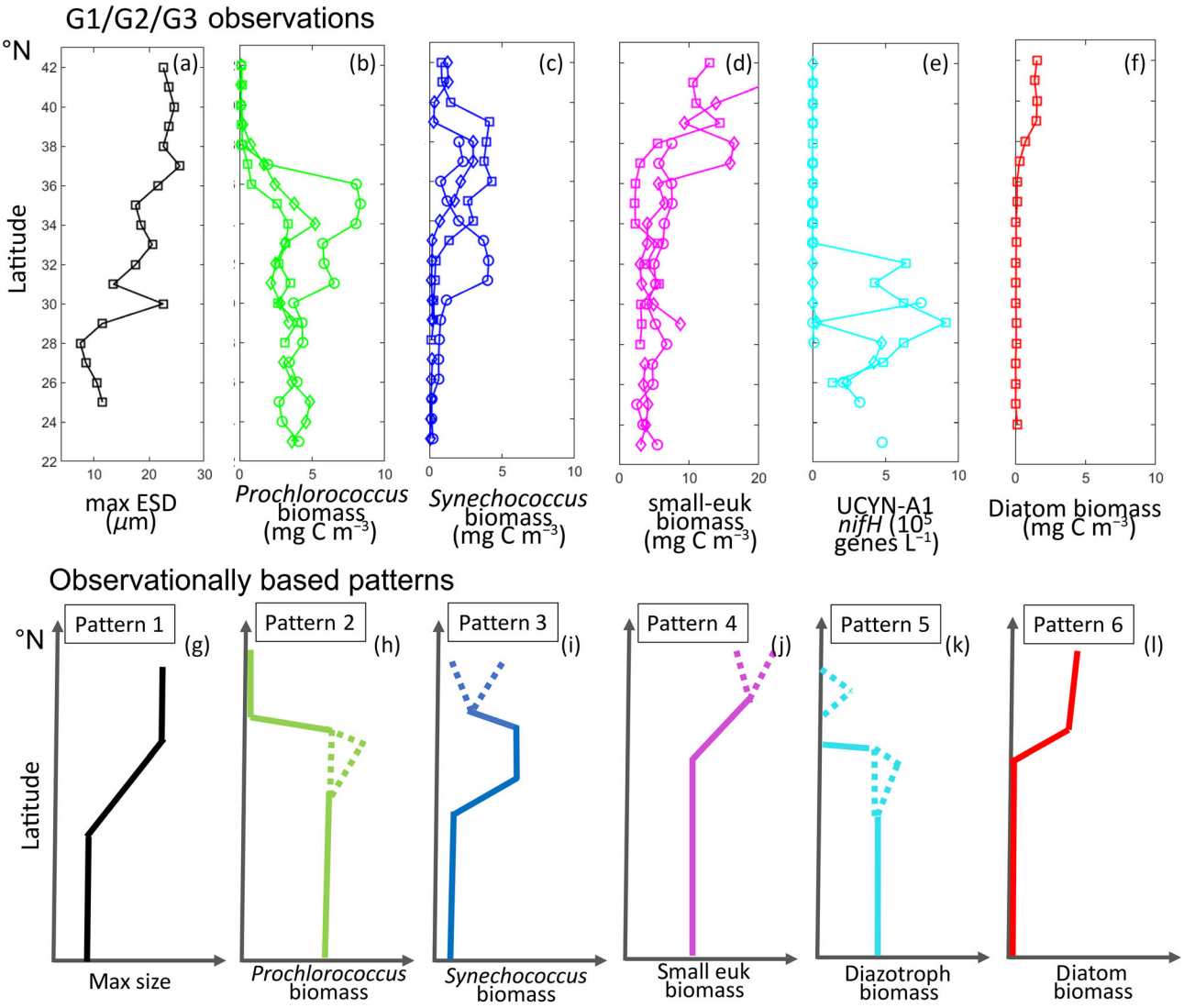

Fig. 2. Patterns: (**a–f**) Observations of phytoplankton communities from surface waters (5–7 m) during G1, G2, and G3, averaged into 1° latitude bins. (**a**) ESD (μm) of 90 percentile of the largest-sized phytoplankton imaged by IFCB (*see* below and Supporting Information Text S1.1); (b) *Prochlorococcus* biomass (mg C m^{-3}); (**c**) *Synechococcus* biomass (mg C m^{-3}); (**d**) small (ESD < 3 μm) eukaryote biomass (mg C m^{-3}); (e) *nifH* gene copies abundance of the diazotroph UCYN-A (10^5 genes L^{-1}); (**f**) diatom biomass (mg C m^{-3}). Circles indicate G1, squares G2, and diamonds G3. Given that rare larger cells are present, for (**a**) we plot the maximum ESD below which 90% of the phytoplankton biomass falls. For (**b**)–(**d**) biomass estimated from light scattering measured by SeaFlow, (**e**) gene copies abundances derived from qPCR, and (**f**) biomass estimated from IFCB. IFCB data was only available for G2. The bottom row (**g–l**) provides schematics highlighting the large-scale patterns deduced from the top row plots; solid lines indicate robust patterns, dashed lines indicate patterns that differ between cruises. *See* Supporting Information Text S1.3 for a description of how these qualitative patterns were determined.

(P), herbivorous zooplankton (Z), carnivorous zooplankton (C, that graze only on herbivorous zooplankton), and heterotrophic bacteria (H) along with inorganic resource (R_p) and organic resource (R_h) (symbols defined in Supporting Information Table S1). We take a strictly trait-based approach where the plankton types are described in terms of size, resource requirement, and trophic strategy. For simplicity, we assume that grazing is also strictly size-based: a larger predator consumes a smaller prey. We first write down a set of differential equations (Supporting Information Table S2; Supporting Information Text S2.1) to encapsulate these simplified ecological interactions (e.g., predator–prey interactions). We then solve these equations in a steady state (i.e., no change of biomass over time) for the resource concentration and biomass of each plankton type (Supporting Information Table S3). In this way, we gain insight into when different plankton types can coexist or not (labeled "insight" in Supporting Information Table S3). We consider what these solutions suggest about the coexistence of biomass patterns along an axis of resource (e.g., inorganic nutrients) supply rate (S_{Rp}). This approach is

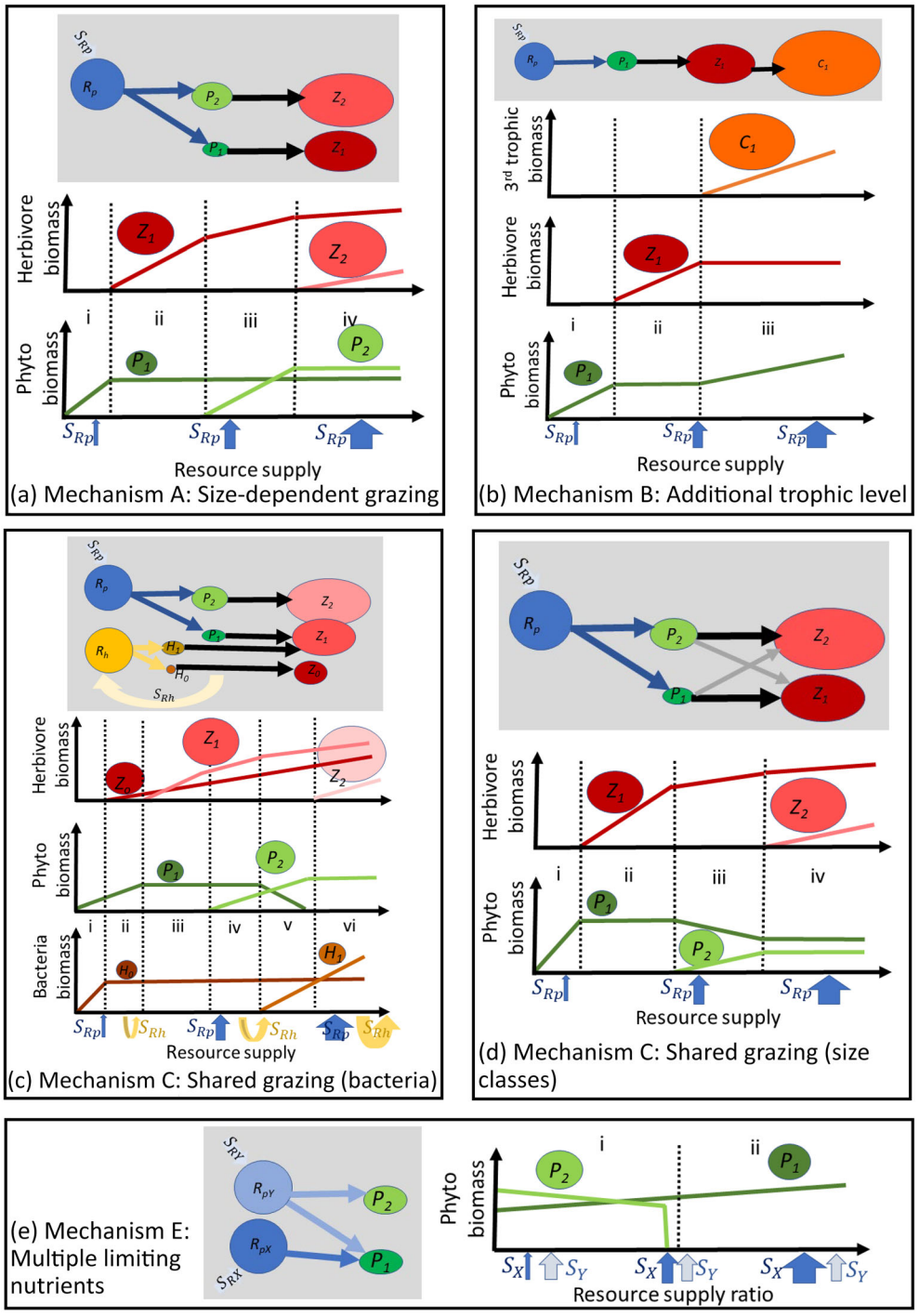

Fig. 3. Mechanisms A–E (*see* Supporting Information Tables S1–S3): Cartoon (gray shaded area) of the ecosystem components used in each of the theoretical frameworks, and schematic graphs indicating the patterns of plankton biomass across a gradient of inorganic resource supply rate (S_{Rp}) as suggested by the theoretical frameworks in steady state (Supporting Information Table S3). The interactions occur between phytoplankton (P), herbivorous zooplankton (Z), carnivorous zooplankton (C), and heterotrophic bacteria (H) along with inorganic resource (R_p) and organic resources (R_h). S_{Rh} is the rate of supply of organic resources. Symbols are defined in Supporting Information Table S1. The relative amount of biomass in each steady-state solution will differ depending on the parameters chosen, as such, the schematics are designed to provide overall patterns across the resource supply rate gradient. The smallest number of plankton types required to explain the theory are used here, but each theory can be extended to include many more size classes/types.

relevant for the North East Pacific Transition Zone, as it ranges from oligotrophic conditions (low supply rate) to high (seasonal) resource supply rates in the north (Fig. 1e). The different frameworks and the insight obtained are shown schematically in Figure 3.

Numerical model

We additionally use a mechanistic numerical model. The model is based on differential equations describing our best understanding of the dynamics at play in the physics, biogeochemistry, and ecology of the ocean. These equations are discretized and stepped forward in time computationally and, as such, the model results are never in a steady state. Specifically, we use the Darwin ecosystem model configured to include the cycling of elements through inorganic, dissolved and particulate detrital pools and 50 plankton types (Fig. 4). The phytoplankton span across 15 size classes and multiple functional groups including diatoms, coccolithophores, prokaryotes, picoeukaryotes (equivalent spherical diameter, ESD $< 2\,\mu$m), diazotrophs, and mixotrophic dinoflagellates. There are 16 size classes of zooplankton and 3 size classes of heterotrophic bacteria. This complex ecosystem, along with inorganic, dissolved, and particulate material, is transported within a three-dimensional global ocean model (MITgcm; Marshall et al. 1997; Wunsch and Heimbach 2007). This specific model setup was previously used in Follett et al. (2022), and the large-scale global distribution and seasonality of bulk ecosystem properties such as Chl *a*, as well as distributions of size classes and functional groups, are plausible in comparison with satellite and in situ observations (*see* supplement of Follett et al. 2022). For more details, *see* Supporting Information Text S3.1. Nutrient fluxes, as shown in Figure 1f, are calculated from the model as discussed in Supporting Information Text S3.2. We conducted a series of numerical model sensitivity experiments to test each of Mechanisms A–E examined in the theoretical frameworks. These experiments are named relative to the mechanism (A–E) that they are targeting (summarized in Supporting Information Table S4).

Results

Observations of community structure

In all three cruises, SeaFlow results showed that the smallest Chl *a*-containing organism (*see* Supporting Information Fig. S1 for relative sizes), the picocyanobacterium *Prochlorococcus*, contributed a large portion of the total phytoplankton biomass in the southern portions of the transects, had relatively uniform distributions to the south, and declined to zero biomass further north (e.g., between 33°N and 36°N depending on the year; Fig. 2b; Supporting Information Fig. S2). This decline to absence of cells occurred sharply (defined here to be a change of more than two standard deviations over 1° latitude, *see* Supporting Information Text S1.3). The next smallest phytoplankter, the pico-cyanobacterium *Synechococcus*, had low biomass in the southern part of the transect, increasing (by more than one standard deviation, *see* Supporting Information Text S1.3) between 30°N and 34°N and decreasing further north (Fig. 2c).

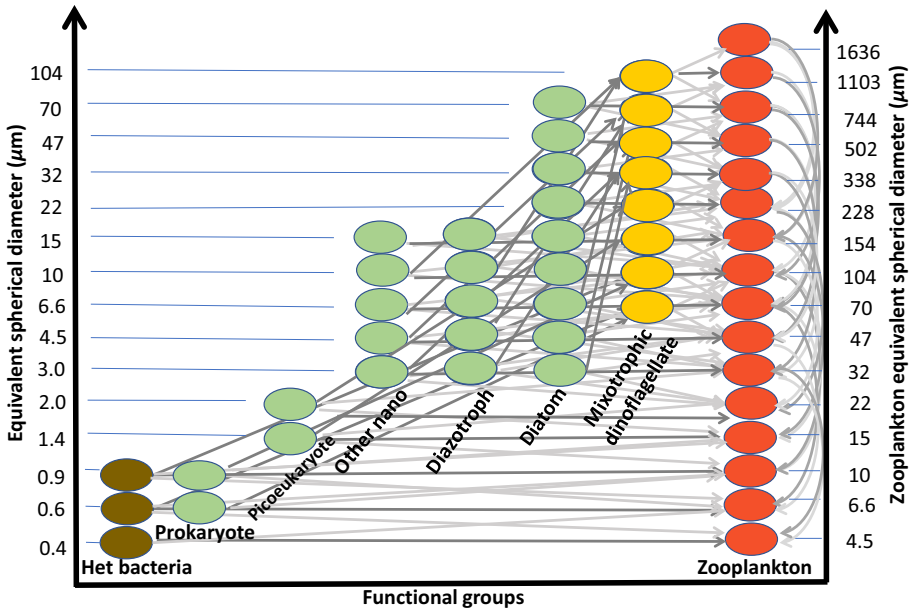

Fig. 4. Schematic of the numerical model ecosystem with plankton arranged by size classes in rows, and functional groups in columns. Note that zooplankton are arranged in the same row as their 10 times smaller prey. Arrows indicate the predator–prey interactions; dark arrows for preferential grazing and lighter for less preferred prey (cross-size grazing). Carnivory is indicated through the curved arrows on the right-hand side. Note that zooplankton that prey on other zooplankton in the model are omnivores, as they also typically prey on phytoplankton.

Small eukaryotes, a diverse set of organisms including picoeukaryotes (ESD < 2 μm) as well as some small nanophytoplankton (ESD 2–3 μm), formed a substantial and stable fraction of the biomass in the southern portion of the transect (sometimes similar in magnitude to *Prochlorococcus*, Supporting Information Fig. S2), and increased in the northern portion (Fig. 2d; Supporting Information Fig. S2). The distribution of the gene marker for nitrogen-fixing organisms, diazotrophs, showed a similar pattern to the picocyanobacteria: The most dominant diazotroph along this transect, UCYN-A, identified by its *nifH* gene (Gradoville et al. 2020), had a sharp decline between 28°N and 33°N depending on the cruise (Fig. 2e). This pattern was also mirrored by the less abundant diazotroph, *Crocosphaera* (Gradoville et al. 2020, Supporting Information Fig. S3). There are suggestions of isolated low abundances of *Crocosphaera* further north, as observed from cell counts, but also *nifH* genes (Gradoville et al. 2020). IFCB measurements, only available for G2, revealed a distinct pattern in diatom distributions: minimal biomass in the southern part of the transect and increasing toward the north (Fig. 2f). Similar patterns of notable increases in diatoms poleward have been observed in previous cruises (e.g., Bogorov 1958; Endo et al. 2018), albeit with less spatial resolution.

Optical imagery (both SeaFlow and IFCB) shows a pattern where phytoplankton biomass is predominantly found in smaller size classes toward the southern end of the transect, while larger phytoplankton tend to coexist more prominently toward the northern section (Fig. 2a; Supporting Information Figs S4, S5). Though the IFCB optical imagery is only available for G2, consistent patterns of increased biomass and particulate organic carbon in larger size classes moving northward were observed in all three cruises, as evidenced by LISST measurements (Supporting Information Fig. S4). This shift in phytoplankton size classes has been noted by Juranek et al. (2020).

Differences in the locations of community structure shifts observed between cruises likely reflect seasonal and interannual environmental changes as indicated by variations in Chl *a*, temperature, and nutrients (e.g., Fig. 1). In this discussion, we focus on the robust patterns (schematically shown with solid lines in Fig. 2g–l) rather than the cruise-to-cruise variability. We also note that similar patterns have been observed in previous cruises, though with less spatial resolution or fewer types of measurements (e.g., Polovina et al. 2001; Church et al. 2008; Juranek et al. 2012). These robust patterns are (going from south to north): (1) that small cells dominate the phytoplankton community in the southern part of the transect, with larger plankton becoming more important further north (Fig. 2g); (2) a sharp decline in *Prochlorococcus* (Fig. 2h); (3) a low *Synechococcus* biomass with an increase and (sometimes) subsequent decease (Fig. 2i); (4) an increase in small Chl *a*-containing eukaryotes (Fig. 2j); (5) a sharp decrease in diazotrophs as suggested by *nifH* genes (Fig. 2k); and (6) an increase in diatoms (Fig. 2l).

Theoretical framework of biotic interactions

The simple frameworks discussed in this section are designed to provide insight into a single set of biotic interactions at a time and, in general, have been examined before in previous literature (*see* equations and references in Supporting Information Tables S2, S3). More details and nuances of these mechanisms can be found in that literature and in Supporting Information Text S2.1. Here, we consider how these interactions could impact phytoplankton groups across the North Pacific Transition Zone.

Mechanism A: Size-specific grazing

Here, we consider a system of two phytoplankton (P_j) of different sizes, along with predatory herbivorous zooplankton (Z_j) that we assume graze only on a specific size class (Fig. 3a) along a gradient of resources supply rate (S_{Rp}, *x*-axis in Fig. 3). In the absence of grazers the smaller phytoplankton (P_1), with the highest nutrient affinity, will out-compete the larger phytoplankton (sector i, that is, before the first dashed vertical line, in graph Fig. 3a). When resource supply rates are high enough to sustain sufficient P_1, a herbivorous zooplankton predator (Z_1) can also be supported and the biomass P_1 is capped (sector ii in Fig. 3a). At higher resource supply, with sufficient grazer pressure from Z_1, the two sizes classes can coexist (sector iii, i.e., when R_{p^*1} equals R_{p^*2}; Supporting Information Table S3; Eqs. SA1a,b, SAI). *Summary*: Size-specific grazing allows an increase in the number of size classes that can coexist along a transect of increasing resource supply rates and sets a uniform distribution of each size class once it is under grazer control. This mechanism can, therefore, explain the inclusion of larger size classes in the north of the transect where nutrient supplies are higher, as seen in pattern 1 (Fig. 2a).

Mechanism B: Third trophic level

Here, we consider a framework with a single phytoplankton type, its predator (herbivorous zooplankton), and a third trophic level (carnivorous zooplankton). At a high enough resource supply rate, Z_1 reaches biomass sufficient to support the next trophic level, the carnivore (sector iii in Fig. 3b; Supporting Information Table S3; Eq. SBI). Without a strong grazer control, the phytoplankton biomass can now increase with higher resource supply rates. *Summary*: When nutrient supply rates are high enough to support a third trophic level (carnivory), the release of grazing pressure allows phytoplankton biomass to increase. This mechanism can explain some of the sharp increases observed along the transition zone (e.g., small eukaryotes, Fig. 2d).

Mechanism C: Shared predation with heterotrophic bacteria

We again consider two size classes of phytoplankton along with their grazers, but now also include two size classes of

heterotrophic bacteria. Phytoplankton consume the inorganic nutrient (R_p) and produce the organic resource (R_h) that fuels the heterotrophic bacteria. As total plankton biomass increases along a gradient of inorganic resource supply rate, the supply of the organic resource also increases. At high enough organic resource supply rates, the larger bacteria (H_1) can be supported (sectors v and vi). In the process of shared predation (also known as "apparent competition," Holt 1977; Holt and Bonsall 2017), the combined biomass of P_1 and H_1 has a uniform concentration (Supporting Information Table S3, Eq. SC3). Thus, as the biomass of H_1 increases, P_1 biomass must decrease (sector v) and eventually reaches zero (sector vi). *Summary*: Shared predation with a similar-sized heterotrophic bacterium can lead to the decline and eventual collapse of that phytoplankton size class with an increasing supply of inorganic (and hence organic) resources. This mechanism can explain the sharp decrease of, for instance, *Prochlorococcus* (Fig. 2b) across the transition zone.

Mechanism D: Shared predation through cross-size grazing

Though grazers appear to have a preference for a certain prey size (Fenchel 1987; Hansen et al. 1997; Kiørboe 2019), they also graze across several size classes, though not all with the same preference (Hansen et al. 1994). Here, we allow multiple zooplankton to graze on a single phytoplankton size class. We call this "cross-size class grazing" and introduce the symbol ϕ, which describes the degree of palatability of a phytoplankton type to a zooplankton type (preferred prey $\phi = 1$, less preferred prey has $\phi < 1$). Once the nutrient supply rate is high enough to support P_2, P_1 decreases (sector iii, *see* also Supporting Information Fig. S6): Shared grazing by the single zooplankton leads to a cap in the combined biomass of the two phytoplankton types. *Summary*: Shared predation, though cross-size class grazing, alters the relative abundance of different size classes and can lead to the exclusion of one size class. This mechanism can explain how a size class (e.g., *Synechococcus*, Fig. 2c) could have low biomass relative to other classes.

Mechanism E: Different limiting resources

The four previous mechanisms focused on when different size classes of phytoplankton could coexist (or not). Here, we instead focus on when two phytoplankton types (the same size or not) can coexist if they are limited by different resources, X_p and Y_p (Fig. 3E). We consider a faster-growing phytoplankton P_1 limited by X_p, but which requires both X_p and Y_p and a slower growing phytoplankton P_2 which only requires Y_p. Here, the theory suggests that coexistence occurs when the ratio of the two resources supply rates (S_Y /S_X, where resource X_p is limiting the faster grower) is in excess of the faster-growing phytoplankton's requirements (γ_{XY1}), as indicated in Eq. SEI (sector i, in Fig. 3e). *Summary*: Two phytoplankton types limited by different resources can coexist if the ratio of the supply rates between the two resources (slower grower limiting resource to faster grower limiting resource) is in excess of the faster-growing phytoplankton's stoichiometric requirements for those two resources. This mechanism can explain where diazotrophs coexist with non-diazotrophs and non-diatoms with diatoms across the transition zone.

Each mechanism discussed above has been considered independently, but in fact, all mechanisms are at play in the real ocean, and the mechanisms likely interact with one another in a nonlinear manner. It becomes intractable to develop a framework that includes all components together along with additional trophic strategies. Even if possible, such a setup would rapidly lose the benefit of theoretical constructs: the clarity that comes from simplicity. In addition, other environmental factors, such as temperature and light, impact growth and grazing rates. These, too, lead to complexity that is difficult to incorporate in a useful theoretical framework.

Numerical model experiments to explore biotic interactions

As a next step in this study, we utilize the numerical (or computational) mechanistic global model of the ocean and its ecosystem. Our numerical model includes all the interactions described by the theoretical frameworks (*see* Supporting Information Table S2), but is significantly more complex. It includes plasticity in trophic levels, many size classes (Fig. 4), multiple limiting nutrients, and growth that is also impacted by light and temperature. In addition, resources and plankton are transported within a three-dimensional moving ocean, with seasonally varying forcing, and are therefore never in a steady state. Our initial simulation (termed the "default", EXP-0, to differentiate it from the sensitivity experiments discussed below) shows patterns across the North East Pacific (Fig. 5a) that are consistent with the observations (Fig. 2): a sharp drop-off of *Prochlorococcus* and diazotrophs toward the north; relatively uniform picoeukaryotes in the south with a sharp increase in the middle of the domain; and almost no diatoms to the south with a sharp increase in the middle of the domain. In the southern portion of the domain, only a few size classes coexist, but many larger size classes coexist further north (Fig. 5a, right panel).

Each of the sensitivity experiments that we discuss next (Supporting Information Table S4) highlights one of the mechanisms A–E (as denoted by experiment name, e.g., EXP-A focused on mechanism A, size-specific grazing) and is compared to the "default" experiment (EXP-0) in terms of phytoplankton community structure. We describe how these expand our understanding relative to the simple theoretical frameworks discussed in the previous section. For additional details and nuances, *see* Supporting Information Text S3.3.

EXP-A: Single generalist grazer

This experiment was designed to explore mechanism A and how size-dependent grazing allows for multiple size classes to coexist. In EXP-A, instead of a range of size classes of zooplankton (as in EXP-0), we have a single zooplankton type that grazes indiscriminately on all size classes of plankton (phytoplankton and bacteria). The number of size classes that

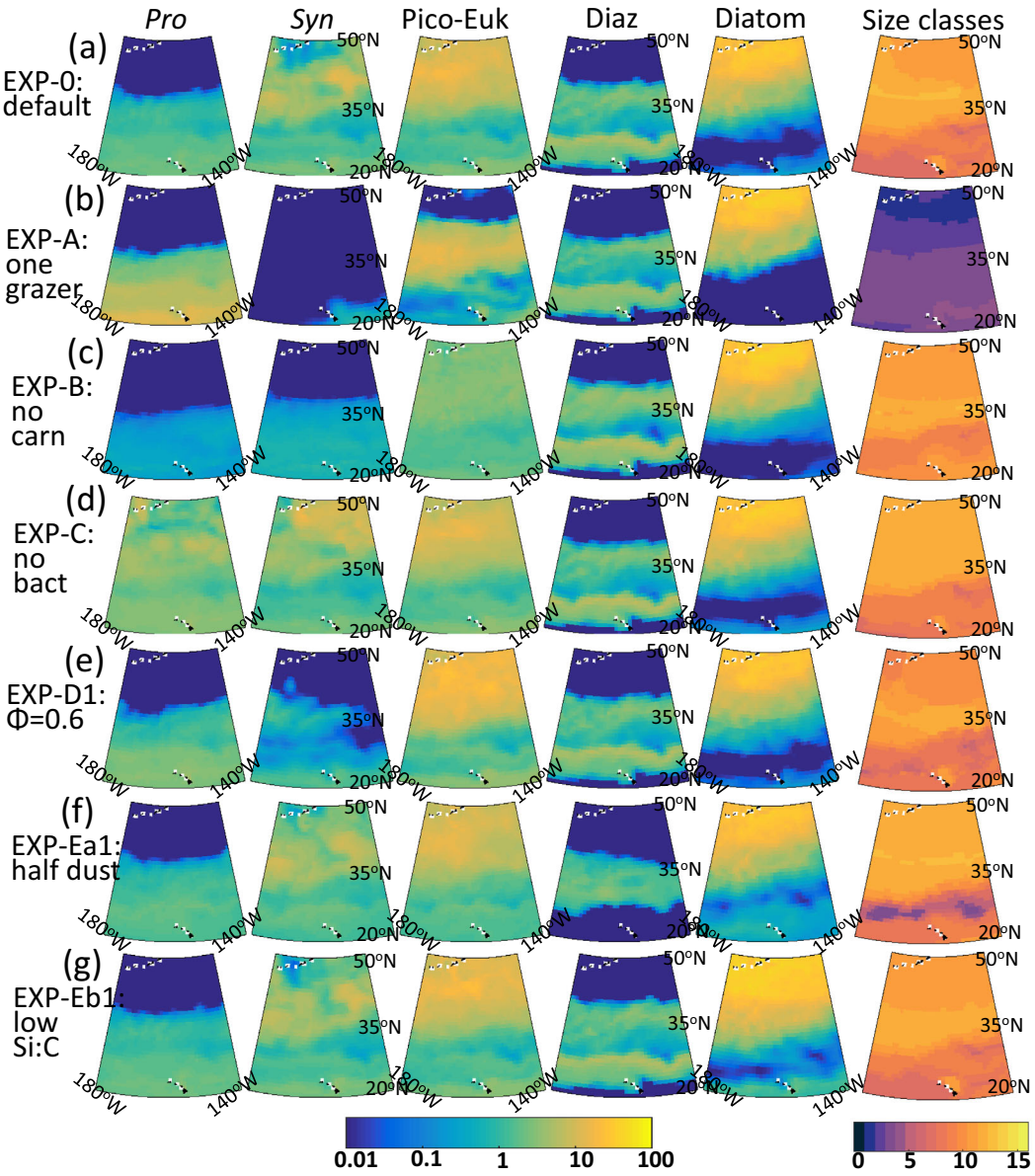

Fig. 5. Modeled annual mean biomass (surface, 0–10 m) of *Prochlorococcus*, *Synechococcus*, picoeukaryotes, diazotrophs, and diatoms (mg C m^{-3}) and (right most column) number of coexisting phytoplankton size classes for experiments: (**a**) EXP-0 (the default); (**b**) EXP-A (single generalist grazer); (**c**) EXP-B (no carnivory); (**d**) EXP-C (no explicit bacteria); (**e**) EXP-D1 (higher cross-size class grazing); (**f**) EXP-Ea1 (low eolian iron deposition); (**g**) EXP-Eb1 (lower requirements of silica in diatoms). Difference plots relative to the default (EXP-A) are shown in Supporting Information Fig. S8. Results from additional experiments are also shown in Supporting Information Figs. S9 (EXP-D2), S11 (EXP-Ea2), and S12 (EXP-Eb2). Here, we show results only for the North East Pacific, but the model is global (*see*, for instance, Supporting Information Fig. S11).

coexist drops dramatically (Fig. 5b, right panel), suggesting that this mechanism is important in maintaining size diversity. However, the number of size classes does not reduce to just the smallest, indicating that other mechanisms can also maintain some level of size diversity (*see* Discussion).

EXP-B: No third trophic level

This experiment was designed to explore whether carnivory allows for increases in biomass as observed for some phytoplankton types across the transect (e.g., picoeukaryotes, Fig. 2d). In EXP-B we do not allow zooplankton to graze on other zooplankton (e.g. removing all the curved arrows in Fig. 4). In this experiment, modeled picoeukaryote biomass is almost uniform across the entire region (Fig. 5c, third panel), in sharp contrast to the default experiment with carnivory (EXP-0). However, diazotroph and diatom patterns do not change much between experiments, suggesting other mechanisms control their distribution.

EXP-C: No explicit bacteria

This experiment was designed to show that shared grazing with a similar-sized heterotrophic bacterium could lead to the poleward collapse of *Prochlorococcus* (mechanism C). In EXP-C, bacteria are not modeled explicitly, but rather remineralization is treated as a rate dependent process. In this experiment, without sharing a grazer with bacteria, *Prochlorococcus* exists across the entire domain (Fig. 5d, left panel). Also noticeable during EXP-C is that in the far north *Synechococcus* (second panel) biomass increases significantly as well, suggesting that shared grazing with the heterotrophic bacteria also limits the *Synechococcus* domain.

EXP-D: Cross-size class grazing

In the default experiment, grazers preferentially ($\phi = 1$) grazed on prey 10 times smaller than themselves, but also grazed on one size class smaller and larger with the preference of $\phi = 0.3$ (*see* Fig. 4). We consider the impact of increasing the cross-size grazing ($\phi = 0.6$) in EXP-D1 and removing any cross-size grazing ($\phi = 0$) in EXP-D2 (Fig. 5e; Supporting Information Figs. S7–S9). *Synechococcus* biomass becomes significantly decreased (Fig. 5e, second panel) with the higher cross-grazing (EXP-D1).

EXP-Ea: Altered iron supply

Diazotrophs in the default simulation are found where there is an excess supply of iron and phosphate relative to non-diazotroph needs (*see* Supporting Information Fig. S10e,f). In this region, phosphate is, in general, sufficient to support diazotrophs. We conduct two experiments (EXP-Ea1 and EXP-Ea2) where we halve or double the amount of iron dust that reaches the ocean, respectively (Fig. 5f; Supporting Information Figs. S8, S11). This effectively alters the ratio of supply rates of

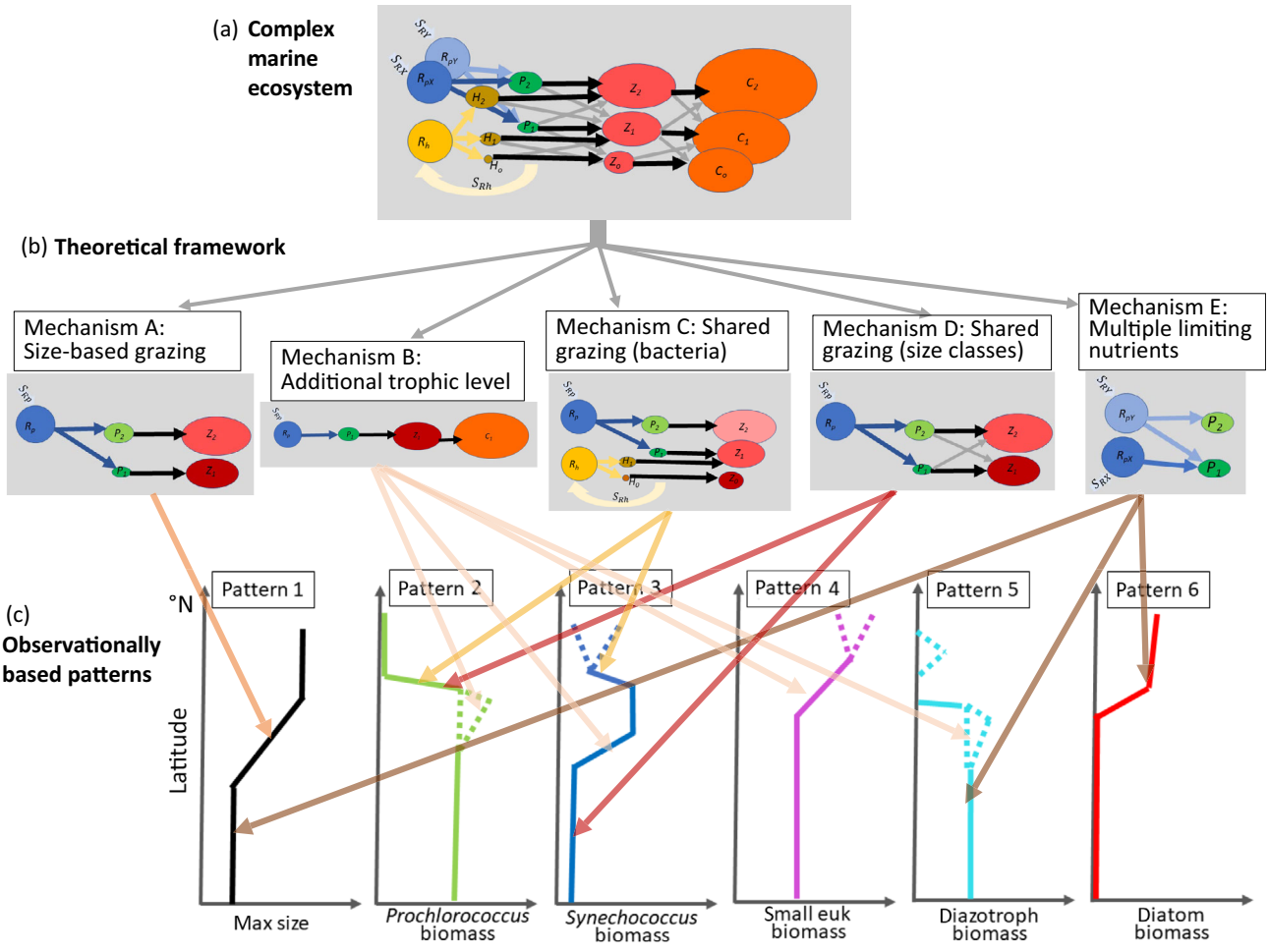

Fig. 6. Summary: (**a**) Marine ecosystems consist of a complex combination of competitive and trophic interactions; (**b**) we separate this complexity into several key "mechanisms" (labeled A–E) and explored these first from a theoretical basis, and then with targeted experiments with a complex computer model that includes all these (and other) processes. We show that a combination of these mechanisms (arrows between panels **b** and **c**) control the (**c**) "patterns" of phytoplankton distributions observed in the SCOPE-Gradients Cruises. Note that (**c**) are the same plots as in Fig. 2g–l, and (**b**) shows the same frameworks as in Fig. 3. The interactions occur between phytoplankton (*P*), herbivorous zooplankton (*Z*), carnivorous zooplankton (*C*), and heterotrophic bacteria (*H*), including their consumption of inorganic resource (R_p), and organic resources (R_h). Symbols are defined in Supporting Information Table S1.

Fe to N (S_{Fe} : S_N) and dramatically changes the biogeography of diazotrophs. There is also an alteration in the diatom distribution (Supporting Information Fig. S11, *see* Discussion).

EXP-Eb: Altered silica requirements for diatoms

We additionally consider two experiments where we alter the stoichiometric demands for silica relative to nitrogen (γ_{SiN}) for diatoms (EXP-Eb1, halved and EXP-Eb2, doubled). Lower γ_{SiN} (EXP-Eb1) leads to more diatoms (Fig. 5g; Supporting Information Figs. S8g, S12). With less utilization of silicic acid in the north, more of this nutrient is transported southward across the region and there is a subsequent extension of the spatial distribution of diatoms relative to the default experiment (EXP-0).

Discussion

Marine food webs have a complex set of competitive and trophic interactions that occur simultaneously (shown schematically in Fig. 6a). We have separated out five different biotic interactions to formally examine each individually within a theoretical framework (Fig. 6b). These interactions are then tested in the more comprehensive mechanistic global model. Our holistic approach demonstrates that the intricate pattern of community structure observed during the SCOPE-Gradients cruises can be understood through multiple interacting mechanisms (schematically shown by multiple arrows between panels b and c in Fig. 6) rather than by only a single mechanism operating in isolation:

1. Size class distribution: The observations suggest that nutrient supply rates, even in the southern portion of the transect, can support several size classes with the two smallest types (*Prochlorococcus*, *Synechococcus*) as well as picoeukaryotes and some nanophytoplankton coexisting (Fig. 2, Supporting Information Fig. S2). As we transit northward across the transect, higher nutrient supply rates support more grazer control, allowing even larger phytoplankton size class to coexist with the smaller classes (mechanism A, size-specific grazing, Fig. 2a; Supporting Information Fig. S4, S5). However, large enough ratios of nutrient supplies, in particular iron vs. nitrogen, can also lead to different size classes coexisting (e.g., the small cells and the slightly larger diazotrophs in the south part of the transition zone). Here, it is the different needs for nutrients (mechanism E, multiple limiting nutrients) rather than grazing pressure that allows the coexistence. Thus, it is a combination of resource competition, size-specific grazing, and different limiting nutrients that control the number of size classes that can coexist.
2. *Prochlorococcus* distribution: In the southern part of the transect, *Prochlorococcus* biomass is controlled/capped by its grazer and remains relatively uniform (mechanism A, size-specific grazing). In the transition zone where resource supply increases rapidly northward, the coexistence of omnivores preying on *Prochlorococcus*' herbivorous grazers can lead to an increase in *Prochlorococcus* (mechanism B, third trophic level), as is seen in some of the cruises. However, shared grazing with similar-sized copiotrophic heterotrophic bacteria (mechanism C) and other size classes of phytoplankton (mechanism D) leads to the ultimate decline of *Prochlorococcus*. Whether the coexistence of the omnivore occurs before or after the critical biomass of plankton sharing the grazer(s) determines whether an increase in *Prochlorococcus* occurs before its decline. This can explain why, in the observations, there is sometimes an increase in *Prochlorococcus* before its decline and sometimes not (Fig. 2b).
3. *Synechococcus* distribution: Theory and model simulations suggest that a relative amount of shared grazing with other size classes of plankton can lead to lower *Synechococcus* biomass in the southern portion of the transect (mechanism D). The small eukaryotes are (for the most part) the largest phytoplankton size class along the southern part of the transect (at least with any major biomass) and so are themselves freed from higher size class cross-grazing pressure. *Prochlorococcus*, on the other hand, will be protected from cross-grazing since it is on the lowest end of size classes and has additional protection from cross-size class grazing if *Synechococcus* is mostly excluded. Similarly, as described in pattern 2 above, we anticipate a relatively uniform biomass of *Synechococcus* in the southern part of the transect (capped/controlled by herbivorous grazers), and an increase in the transition zone when carnivory reduces this grazing pressure (mechanism B, third trophic level). A decline even further north, seen on two cruises, can be explained by a shared grazer with heterotrophic bacteria and higher size classes of phytoplankton (mechanisms C and D).
4. *Picoeukaryote distribution*: Herbivorous grazing leads to the relatively uniform biomass of picoeukaryotes across the southern part of the transect (mechanism A), and the presence of carnivores further north leads to the abrupt increase in this size class of phytoplankton (mechanism B, third trophic level).
5. *Diazotroph distribution*: The excess supply of iron and phosphate relative to DIN, given the needs of the non-diazotrophs, allows for diazotrophs to exist in the southern portion of the transects. Further north, there is no such excess and there is a sharp decline in diazotroph abundances (mechanism E, multiple limiting nutrients).
6. *Diatom distribution*: Insufficient silica to fulfill diatom stoichiometric requirements (mechanism E, multiple limiting nutrients) in the southern portion of the transect strongly limits the diatom biomass in this region. Silicic acid supply is, however, strongly related to the degree of iron limitation of diatoms upstream (e.g., Equatorial Pacific and Northern Pacific subpolar gyre), and changes in the iron supply could lead to shifts in the diatom biogeography (experiment EXP-Ea; Supporting Information Fig. S11; Supporting Information Text S2.1).

Our study highlights that it is a combination of microbial interactions that alter across a gradient of resource supply rates that are key in understanding coexistence: competition for scarce resources, grazing pressure, and shared grazing with other plankton. Though previous studies have considered some of these mechanisms individually to explain similar types of observed biogeography (e.g., cell size along the Atlantic Meridional Transect, Acevedo-Trejos et al. 2018; Dutkiewicz et al. 2020, or global distribution of nitrogen fixers Ward et al. 2013) this study is unique in synthesizing multiple mechanisms to explain a community of phytoplankton.

Previous observational studies (e.g., Fuhrman 2009; Lima-Mendez et al. 2015) have shown through correlation that biotic interactions appear important in setting community structure. Here, we have shown this mechanistically. We find that the magnitude of the resource supply rate facilitates these different interactions among organisms. The critical values of the supply rate that allows coexistence ("insights" in Supporting Information Table S3) differ in whether they are set by phytoplankton physiological parameters (e.g., mechanism A, Insight SAI), grazing parameters (e.g., mechanisms C and D; Eq. SC3, Insight SDI), or stoichiometric requirements (mechanism E, Insight SEI). Since these parameters may or may not be controlled by the environment (such as photosynthetically available radiation, temperature), the critical values of the supply rates will vary over both time and space scales. For instance, mechanism A (Insight SAI) is a function of maximum phytoplankton growth rate (impacted by temperature and light), while mechanism B is a function of maximum grazing rate (impacted by temperature, but not light). Given these important differences, and because nutrient supply rates vary temporally (*see* Fig. 1f), the features of the increases and decreases in different plankton types should move latitudinally with season (*see* Supporting Information Fig. S13) and interannually, but not necessarily at the same rate. This likely causes some of the differences observed between the three cruises. These results also suggest that abiotic factors (e.g., temperature) alone are unlikely to be able to provide realistic predictions of community structure.

Here, we have considered five mechanisms and the patterns of only a subset of the complex phytoplankton community and trait distributions. However, the ocean is far more complex and includes many more types of organisms (e.g., viruses) and interactions (colony formation, symbiosis, chemical signaling) than discussed here. As such, we view our study as an initial attempt at understanding the first-order, large-picture, patterns. Traits such as buoyancy control, morphology (*see*, e.g., Ryabov et al. 2021), symbiosis, chain/colony formation, and mixotrophy might allow larger size classes to coexist in lower nutrient regions than the theory suggests. Other components of the marine food web, such as higher trophic levels and, in particular, viruses will also interact in ways that are likely important. For instance, Carlson et al. (2022) hypothesized, also using SCOPE-Gradients observations, that viruses can play, at times, a critical role in *Prochlorococcus* distributions. In addition, there are other patterns of community structure (for instance, the latitudinal gradient in mixotrophy, Lambert et al. 2022) across the transition zone that we have not attempted to explain here. Several of the observed picoeukaryotes are mixotrophic (e.g., Li et al. 2022), and how this plasticity in trophic strategy plays out in maintaining size diversity is important to explore in a follow-on study. (Our numerical model only included larger mixotrophic dinoflagellates.) Furthermore, motility might also be an important mechanism to explore: For instance, some picoeukaryotes are motile and this will impact their level of shared grazing with the non-motile cyanobacteria. Our study is holistic, not exhaustive, but does provide clear hypotheses on some of the mechanisms structuring community composition across strong gradients in the supply of resources.

We hypothesize that a combination of biotic interactions driven by size-based growth and grazing; changing lengths of trophic chains; and stoichiometric constraints are needed to explain the bulk compositional patterns in phytoplankton across the North East Pacific Transition Zone. Additional measurements and further analysis could help expand on the mechanisms discussed in this study. For instance, estimates of the patterns in size classes of zooplankton (for mechanism A, size-specific grazing) could be obtained from imaging flow cytometers. Further analysis of metatranscriptome and metagenomic data from G1 to G3 (and other cruises) could provide insights and identify the grazing partners, particularly in community composition and trophic modes of the picoeukaryotes and other groups. In particular, these data might identify the shared grazers in mechanisms D and E. Additional measurements to ascertain the length of food chains and exploration of trophic level of grazers (for mechanism B, third trophic level), higher resolution of heterotrophic bacteria size classes (mechanism C), evaluation of the grazers of the smallest size classes in both field observations and laboratory experiments (mechanism D, cross-size class grazing), and quantification of ratio of supply rate of different nutrients (mechanism E) should be priorities in future plans.

Conclusions

Phytoplankton form the base of the food web and drive the cycling of carbon in the sea. They contain a high diversity of species and form complex spatial–temporal patterns in the environment, which can be difficult to simplify. Our study provides a holistic understanding of the large scale, and yet intricate, patterns of community composition observed in the North East Pacific Transition Zone. We find that it is not enough to examine a single mechanism to explain the observed patterns, but that multiple co-occurring biotic interactions are needed. Such a complete synthesis is essential for us to begin to understand the complexity of the natural world, and the insight it provides is crucial for us to be able to predict

what will happen to phytoplankton communities in a warming world.

We have shown that multiple competitive and trophic interactions work together to establish community structure. Where these biotic interactions occur is set by the gradient in resource supply and in the ratio of multiple resource supplies across the transition zone. The mechanisms suggested by our study are general and likely set community structure across many environmental gradients in the global ocean. Our work provides testable hypotheses, a path for large synthesis efforts, a catalyst for further data analysis, and suggests a cross-gradient observational strategy for fully understanding and predicting plankton community structure in our changing oceans.

Data availability statement

Cruise data are freely available via Zenodo.org. SeaFlow data for G1–G3 used in this study (as well as additional cruises) is available at https://doi.org/10.5281/zenodo.2678021. LISST data for G1-G3 are available at https://doi.org/10.5281/zenodo.7754538. IFCB data is available at https://doi.org/10.5281/zenodo.4267140 and https://doi.org/10.5281/zenodo.4267135. *nifH* gene abundance data for G1 and G2 were published in a supplement of Gradoville et al. (2020) and G3 is available at https://doi.org/10.5281/zenodo.7779671. All data can be accessed and viewed via SimonsCMAP (Ashkezari et al. 2021). The general circulation model (MITgcm) is available through mitgcm.org, and the generic biogeochemical/ecosystem code used in this study is available at https://github.com/darwinproject/darwin3. The specific version and modifications for the setup used here, and all parameter values are freely available through Harvard Dataverse at https://doi.org/10.7910/DVN/SGCZMC. Model output used in this study is available at https://doi.org/10.7910/DVN/5YRVHO.

References

Acevedo-Trejos, E., E. Marañón, and A. Merico. 2018. Phytoplankton size diversity and ecosystem function relationships across oceanic regions. Proc. Biol. Sci. **285**: 20180621. doi:10.1098/rspb.2018.0621

Aiken, J., Y. Pradhan, R. Barlow, S. Lavender, A. Poulton, P. Holligan, and N. Hardman-Mountford. 2009. Phytoplankton pigments and functional types in the Atlantic Ocean: A decadal assessment, 1995–2005. Deep-Sea Res. II: Top. Stud. Oceanogr. **56**: 899–917. doi:10.1016/j.dsr2.2008.09.017

Allen, J. G., M. Dugenne, R. M. Letelier, and A. E. White. 2022. Optical determinations of photophysiology along an ecological gradient in the North Pacific Ocean. Limnol. Oceanogr. **67**: 713–725. doi:10.1002/lno.12031

Armstrong, R. A. 1999. Stable model structures for representing biogeochemical diversity and size spectra in plankton communities. J. Plankton Res. **21**: 445–464. doi:10.1093/plankt/21.3.445

Ashkezari, M. D., and others. 2021. Simons Collaborative Marine Atlas Project (Simons CMAP): An open-source portal to share, visualize and analyze ocean data. Limnol. Oceanogr.: Methods **19**: 488–496. doi:10.1002/lom3.10439

Banas, N. S. 2011. Adding complex trophic interactions to a size-spectral plankton model: Emergent diversity patterns and limits on predictability. Ecol. Model. **222**: 2663–2675. doi:10.1016/j.ecolmodel.2011.05.018

Björkman, K., S. Duhamel, M. Church, and D. Karl. 2018. Spatial and temporal dynamics of inorganic phosphate and adenosine-5′-triphosphate in the North Pacific Ocean. Front. Mar. Sci. **5**: 235. doi:10.3389/fmars.2018.00235

Bogorov, B. G. 1958. Biogeographical regions of the plankton of the North-Western Pacific ocean and their influence on the deep sea. Deep-Sea Res. **5**: 149–161. doi:10.1016/0146-6313(58)90005-4

Boysen, A., and others. 2022. Glycine betaine uptake and metabolism in marine microbial communities. Environ. Microbiol. **24**: 2380–2403. doi:10.1111/1462-2920.16020

Carlson, M., and others. 2022. Viruses affect picocyanobacterial abundance and biogeography in the North Pacific Ocean. Nat. Microbiol. **7**: 570–580. doi:10.1038/s41564-022-01088-x

Cermeño, P., and others. 2016. Marine primary productivity is driven by a selection effect. Front. Mar. Sci. **3**: 173. doi:10.3389/fmars.2016.00173

Church, M. J., K. M. Björkman, D. M. Karl, M. A. Saito, and J. P. Zehr. 2008. Regional distributions of nitrogen-fixing bacteria in the Pacific Ocean. Limnol. Oceanogr. **53**: 63–77. doi:10.4319/lo.2008.53.1.0063

Dutkiewicz, S., P. Cermeño, O. Jahn, M. J. Follows, A. A. Hickman, D. A. A. Taniguchi, and B. A. Ward. 2020. Dimensions of marine phytoplankton diversity. Biogeosciences **17**: 609–634. doi:10.5194/bg-17-609-2020

Endo, H., H. Ogata, and K. Suzuki. 2018. Contrasting biogeography and diversity patterns between diatoms and haptophytes in the central Pacific Ocean. Sci. Rep. **8**: 10916. doi:10.1038/s41598-018-29039-9

Fenchel, T. 1987. Ecology—Potentials and limitations. Excellence in ecology: Book 1. Ecological Institute.

Flombaum, P., W. L. Wang, F. W. Primeau, and A. C. Martiny. 2020. Global picophytoplankton niche partitioning predicts overall positive response to ocean warming. Nat. Geosci. **13**: 116–120. doi:10.1038/s41561-019-0524-2

Flombaum, P., and others. 2013. Present and future global distributions of the marine Cyanobacteria *Prochlorococcus* and *Synechococcus*. Proc. Natl. Acad. Sci. USA **110**: 9824–9829. doi:10.1073/pnas.1307701110

Follett, C. L., S. Dutkiewicz, G. Forget, B. B. Cael, and M. J. Follows. 2021. Moving ecological and biogeochemical transitions across the North Pacific. Limnol. Oceanogr. **66**: 2442–2454. doi:10.1002/lno.11763

Follett, C. L., S. Dutkiewicz, F. Ribalet, E. Zakem, D. Caron, E. V. Armbrust, and M. J. Follows. 2022. Trophic interactions with heterotrophic bacteria limit the range of *Prochlorococcus*. Proc. Natl. Acad. Sci. USA **119**: e2110993118. doi:10.1073/pnas.2110993118

Fremont, P., M. Gehlen, M. Vrac, J. Leconte, T. O. Delmont, P. Wincker, D. Iudicone, and O. Jaillon. 2022. Restructuring of plankton genomic biogeography in the surface ocean under climate change. Nat. Clim. Change **12**: 393–401. doi:10.1038/s41558-022-01314-8

Fuhrman, J. A. 2009. Microbial community structure and its functional implications. Nature **459**: 193–199. doi:10.1038/nature08058

Gradoville, M. R., and others. 2020. Latitudinal constraints on the abundance and activity of the cyanobacterium UCYN-A and other marine diazotrophs in the North Pacific. Limnol. Oceanogr. **65**: 1858–1875. doi:10.1002/lno.11423

Graff van Crevel, S., S. Coesel, S. Blawskowski, R. Groussman, M. Schatz, and E. Armbrust. 2023. Diveregent functions of two clades of flavodoxin in diatoms mitigate oxidative stress and iron limitation. eLife **12**: e84392. doi:10.7554/eLife.84392

Guidi, L., L. Stemmann, G. A. Jackson, F. Ibanez, H. Claustre, L. Legendre, M. Picheral, and G. Gorsky. 2009. Effects of phytoplankton community on production, size and export of large aggregates: A world-ocean analysis. Limnol. Oceanogr. **54**: 1951–1963. doi:10.4319/lo.2009.54.6.1951

Hansen, B., P. K. Bjornsen, and P. J. Hansen. 1994. The size ratio between planktonic predators and their prey. Limnol. Oceanogr. **39**: 395–403. doi:10.4319/lo.1994.39.2.0395

Hansen, P. J., P. K. Bjørnsen, and B. W. Hansen. 1997. Zooplankton grazing and growth: Scaling within the 2-2,000-µm body size range. Limnol. Oceanogr. **42**: 687–704. doi:10.4319/lo.1997.42.4.0687

Heal, K. R., and others. 2021. Marine community metabolomes carry fingerprints of phytoplankton community composition. mSystems **6**: e01334-20. doi:10.1128/msystems.01334-20

Holt, R. D. 1977. Predation, apparent competition, and the structure of prey communities. Theor. Popul. Biol. **12**: 197–229. doi:10.1016/0040-5809(77)90042-9

Holt, R. D., and M. B. Bonsall. 2017. Apparent competition. Annu. Rev. Ecol. Evol. Syst. **48**: 447–471. doi:10.1146/annurev-ecolsys-110316-022628

Juranek, L. W., P. D. Quay, R. A. Feely, D. Lockwood, D. M. Karl, and M. J. Church. 2012. Biological production in the NE Pacific and its influence on air-sea CO_2 flux: Evidence from dissolved oxygen isotopes and O_2/Ar. J. Geophys. Res.: Oceans **117**: C05022. doi:10.1029/2011JC007450

Juranek, L. W., and others. 2020. The importance of the phytoplankton "middle class" to ocean net community production. Glob. Biogeochem. Cycles **34**: e2020GB006702. doi:10.1029/2020GB006702

Kavanaugh, M. T., S. R. Emerson, B. Hales, D. M. Lockwood, P. D. Quay, and R. M. Letelier. 2014. Physicochemical and biological controls on primary and net community production across northeast Pacific seascapes. Limnol. Oceanogr. **59**: 2013–2027. doi:10.4319/lo.2014.59.6.2013

Kiørboe, T. 2019. A mechanistic approach to plankton ecology. Princeton Univ. Press. doi:10.1515/9780691190310

Lambert, B. S., R. D. Groussman, M. J. Schatz, S. N. Coesel, B. P. Durham, A. J. Alverson, A. E. White, and E. V. Armbrust. 2022. The dynamic trophic architecture of open-ocean protist communities revealed through machine-guided metatranscriptomics. Proc. Natl. Acad. Sci. USA **119**: e2100916119. doi:10.1073/pnas.2100916119

Li, Q., K. F. Edwards, C. R. Schvarcz, and G. F. Steward. 2022. Broad phylogenetic and functional diversity among mixotrophic consumers of *Prochlorococcus*. ISME J. **16**: 1751–7370. doi:10.1038/s41396-022-01204-z

Lima-Mendez, G., and others. 2015. Determinants of community structure in the global plankton interactome. Science **348**: 1262073. doi:10.1126/science.1262073

Margalef, R. 1978. Life-forms of phytoplankton as survival alternatives in an unstable environment. Oceanol. Acta **1**: 493–509.

Marshall, J., A. Adcroft, C. Hill, L. Perelman, and C. Heisey. 1997. A finite-volume, incompressible Navier Stokes model for, studies of the ocean on parallel computers. J. Geophys. Res. C: Oceans **102**: 5753–5766. doi:10.1029/96JC02775

Park, J., and others. 2023. Siderophore production and utlization by marine bacteria in the North Pacific Ocean. Limnol. Oceanogr. **68**: 1636–1653. doi:10.1002/lno.12373

Pinedo-Gonźalez, P., and others. 2020. Anthropogenic Asian aerosols provide Fe to the North Pacific Ocean. Proc. Natl. Acad. Sci. USA **117**: 27862–27868.

Polovina, J. J., E. Howell, D. R. Kobayashi, and M. P. Seki. 2001. The transition zone chlorophyll front, a dynamic global feature defining migration and forage habitat for marine resources. Prog. Oceanogr. **49**: 469–483. doi:10.1016/S0079-6611(01)00036-2

Ribalet, F., and others. 2019. SeaFlow data v1, high-resolution abundance, size and biomass of small phytoplankton in the North Pacific. Sci. Data **6**: 277. doi:10.1038/s41597-019-0292-2

Ryabov, A., O. Kerimoglu, E. Litchman, I. Olenina, L. Roselli, A. Basset, E. Stanca, and B. Blasius. 2021. Shape matters: The relationship between cell geometry and diversity in phytoplankton. Ecol. Lett. **24**: 847–861. doi:10.1111/ele.13680

Schlosser, C., and others. 2013. Seasonal ITCZ migration dynamically controls the location of the (sub)tropical Atlantic biogeochemical divide. Proc. Natl. Acad. Sci. USA **111**: 1438–1442. doi:10.1073/pnas.131867011

Tang, W., and N. Cassar. 2019. Data-driven modeling of the distribution of diazotrophs in the global ocean. Geophys. Res. Lett. **46**: 12258–12269. doi:10.1029/2019GL084376

Tréguer, P., and others. 2018. Influence of diatom diversity on the ocean biological carbon pump. Nat. Geosci. **11**: 27–37. doi:10.1038/s41561-017-0028-x

Ward, B. A., S. Dutkiewicz, C. M. Moore, and M. J. Follows. 2013. Iron, phosphorus, and nitrogen supply ratios define the biogeography of nitrogen fixation. Limnol. Oceanogr. **58**: 2059–2075. doi:10.4319/lo.2013.58.6.2059

Ward, B. A., S. Dutkiewicz, and M. J. Follows. 2014. Modelling spatial and temporal patterns in size-structured marine plankton communities: Top-down and bottom-up controls. J. Plankton Res. **36**: 31–47. doi:10.1093/plankt/fbt097

White, A., A. Whitmire, B. Barone, R. Letelier, D. Karl, and M. Church. 2015. Phenology of particle size distributions in the North Pacific gyre (Station ALOHA). J. Geophys. Res.: Oceans **120**: 7381–7399. doi:10.1002/2015JC010897

Wunsch, C., and P. Heimbach. 2007. Practical global oceanic state estimation. Phys. D: Nonlinear Phenom. **230**: 197–208. doi:10.1016/j.physd.2006.09.040

Xu, Z., and others. 2022. Disentangling the ecological processes shaping the latitudinal pattern of phytoplankton communities in the Pacific Ocean. mSystems **7**: e0120321. doi:10.1128/msystems.01203-21

Acknowledgments

This work was supported by the Simons Collaboration on Ocean Processes and Ecology Gradients (SCOPE-Gradients) (Grant IDs: DMK 721252, EVA 426570SP and 721244, MJF 329108, AEW 329104 and 721256) and the Simons Collaboration on Computational Biogeochemical Modeling of Marine Ecosystem (CBIOMES) (Grant IDs: AJI 549935, ZVF 549937, SD, OJ, MJF 549931, JPM 459949, EVA, FR 549945, CLF 827829). We thank the editors and an anonymous reviewer for their valuable comments.

Conflict of Interest

The all other authors declare that they have no competing interests.

Submitted 02 July 2023
Revised 13 February 2024
Accepted 07 March 2024

Associate editor: C. Elisa Schaum